LIM and cysteine-rich domains 1 is required for thrombin-induced smooth muscle cell proliferation and promotes atherogenesis

Received for publication, November 8, 2017, and in revised form, January 9, 2018 Published, Papers in Press, January 11, 2018, DOI 10.1074/jbc.RA117.000866

Jagadeesh Janjanam[‡], Baolin Zhang[‡], Arul M. Mani[‡], Nikhlesh K. Singh[‡], James G. Traylor, Jr.[§], A. Wayne Orr[§], and Gadiparthi N. Rao[‡1]

From the [‡]Department of Physiology, University of Tennessee Health Science Center, Memphis, Tennessee 38163 and the [§]Department of Pathology, Louisiana State University Health Sciences Center, Shreveport, Louisiana 71103

Edited by George M. Carman

Restenosis arises after vascular injury and is characterized by arterial wall thickening and decreased arterial lumen space. Vascular injury induces the production of thrombin, which in addition to its role in blood clotting acts as a mitogenic and chemotactic factor. In exploring the molecular mechanisms underlying restenosis, here we identified *LMCD1* (LIM and cysteine-rich domains 1) as a gene highly responsive to thrombin in human aortic smooth muscle cells (HASMCs). Of note, LMCD1 depletion inhibited proliferation of human but not murine vascular smooth muscle cells. We also found that by physically interacting with E2F transcription factor 1, LMCD1 mediates thrombin-induced expression of the CDC6 (cell division cycle 6) gene in the stimulation of HASMC proliferation. Thrombin-induced LMCD1 and CDC6 expression exhibited a requirement for protease-activated receptor 1-mediated $G\alpha_{q/11}$-dependent activation of phospholipase C β3. Moreover, the expression of LMCD1 was highly induced in smooth muscle cells located at human atherosclerotic lesions and correlated with CDC6 expression and that of the proliferation marker Ki67. Furthermore, the LMCD1- and SMCαactin-positive cells had higher cholesterol levels in the atherosclerotic lesions. In conclusion, these findings indicate that by acting as a co-activator with E2F transcription factor 1 in CDC6 expression, LMCD1 stimulates HASMC proliferation and thereby promotes human atherogenesis, suggesting an involvement of LMCD1 in restenosis.

Restenosis, characterized by arterial wall thickening and decreased arterial lumen space, occurs as a response to vascular injury (1, 2). Vascular smooth muscle cell (VSMC)[2] migration and proliferation in the tunica intima is the root cause of restenosis (1–3). Vascular injury stimulates coagulation cascade activation and produces substantial amounts of thrombin (4). The thrombus formed because of injury can serve as a reservoir of active thrombin (5). Thrombin, in addition to its vital role in blood clotting, acts as a mitogen and chemotactic factor to a variety of cell types, including peripheral blood monocytes and VSMCs (6–8). In identifying the thrombin-induced genes by microarray analysis, we found that a novel LMCD1 (LIM and cysteine-rich domains 1) gene was induced by thrombin in a sustained manner in human aortic smooth muscle cells (HASMCs). LMCD1, a member of the LIM protein family, contains a novel cysteine-rich domain at the N terminus, a central PET (Prickle, Espinas, and Testin) domain, and two LIM domains at the C-terminal region (9). The proteins containing LIM domains are known to have distinct functions in gene expression, cell adhesion, cytoskeleton remodeling, and signal transduction (10). Although the cellular functions of many LIM proteins have been studied (10), there are only a limited number of reports on the biological functions of LMCD1. It was reported that LMCD1 plays a role in the development of cardiac hypertrophy (11). Another study suggests that LMCD1 acts as a transcriptional repressor for GATA6, a zinc-finger transcription factor, in lung and cardiac tissues (12). Previous studies indicate that GATA6 mediates the expression of both SMC synthetic genes such as endothelin-1 and quiescent genes such as $p21^{Cip1}$ (13, 14). Because LMCD1 is identified as a novel gene induced by thrombin and we know that thrombin promotes VSMC proliferation, we asked the question of whether LMCD1 mediates thrombin-induced HASMC proliferation, and if so, what could be the possible mechanism, which is the major goal of this current study. In the present study, we report that LMCD1 acts as a co-activator for E2F1 in the modulation of thrombin-induced CDC6 expression in promoting HASMC replication.

Results

To identify thrombin-induced genes in HASMCs, we have performed microarray analysis and identified 47 genes that were up-regulated above 2-fold in response to thrombin (0.5

This work was supported by NHLBI, National Institutes of Health Grants HL069908 and HL103575 (to G. N. R.) and HL098435 and HL133497 (to A. W. O.). The authors declare that they have no conflicts of interest with the contents of this article. The content is solely the responsibility of the authors and does not necessarily represent the official views of the National Institutes of Health.

[1] To whom correspondence should be addressed: Dept. of Physiology, University of Tennessee Health Science Center, 71 S. Manassas St., Memphis, TN 38163. Tel.: 901-448-7321; Fax: 901-448-7126; E-mail: rgadipar@uthsc.edu.

[2] The abbreviations used are: VSMC, vascular smooth muscle cell; HASMC, human aortic smooth muscle cell; MASMC, mouse aortic smooth muscle cell; RASMC, rat aortic smooth muscle cell; E2F1, E2F transcription factor 1; PAR1, protease-activated receptor 1; PLC, phospholipase C; EMSA, electrophoretic mobility shift assay; ORC, origin recognition complex; nt, nucleotide(s); PLA, proximal ligation assay; PDGF, platelet-derived growth factor; HRP, horseradish peroxidase; BI, balloon injury; CAL, carotid artery ligation.

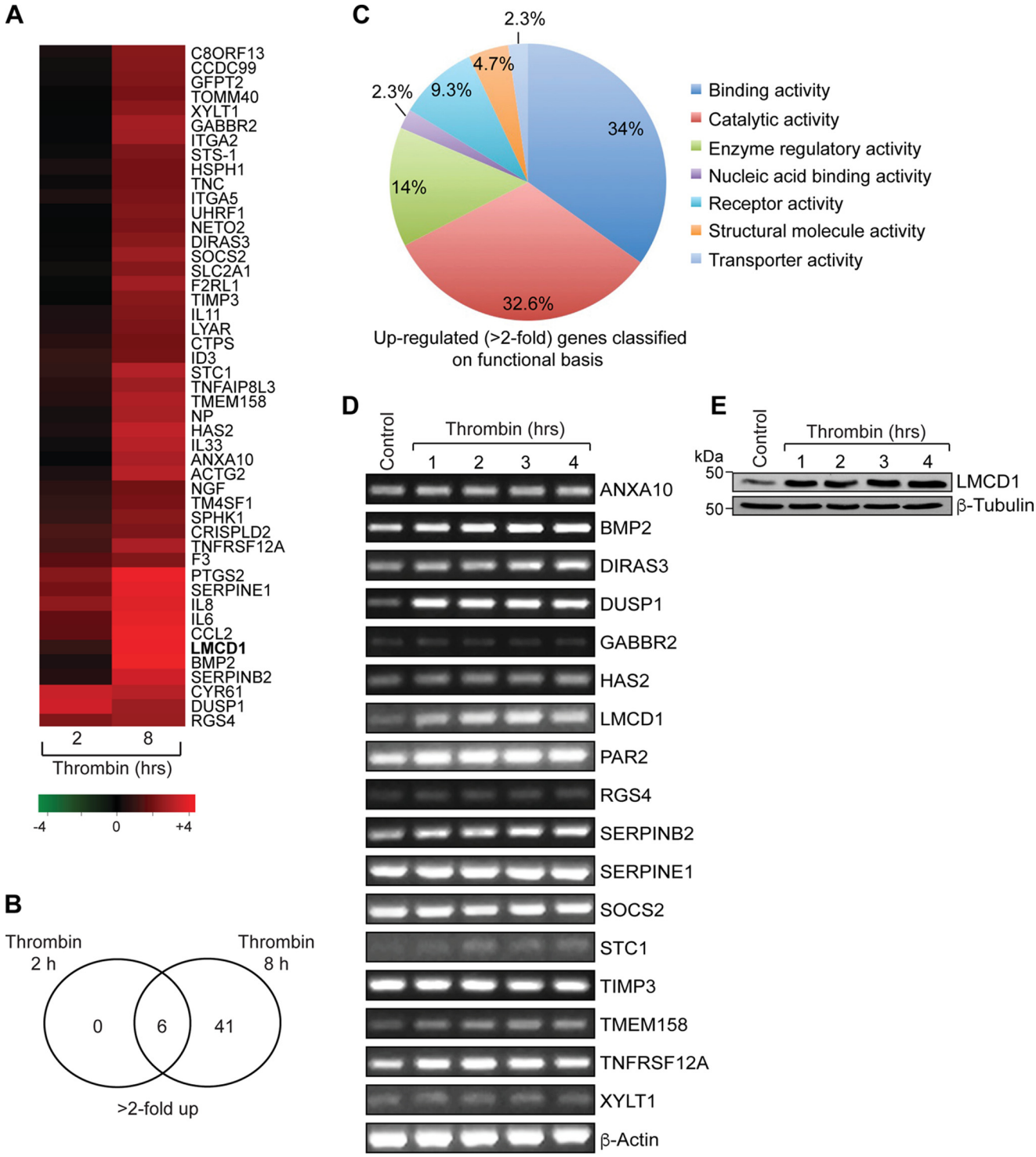

Figure 1. Microarray analysis shows LMCD1 as a highly responsive gene to thrombin in HASMCs. *A*, quiescent HASMCs were treated with and without thrombin (0.5 unit/ml) for 2 and 8 h. Total cellular RNA was isolated from control and the thrombin-treated cells and subjected to microarray analysis. Thrombin-induced genes that were up-regulated by more than 2-fold are presented as a heat map. *B*, Venn diagram showing the number of genes that were up-regulated by more than 2-fold at both 2 and 8 h of thrombin treatment as compared with control. *C*, gene ontology analysis of the thrombin-induced genes based on their molecular function. *D*, quiescent HASMCs were treated with and without thrombin (0.5 unit/ml) for various time periods, and total cellular RNA was isolated. Equal amounts of RNA from control and each treatment were analyzed by RT-PCR for the indicated genes using their specific primers. *E*, all the conditions were same as in *D* except that after the indicated treatments, the cell extracts were prepared, and equal amounts of protein from control and each treatment were analyzed for LMCD1 levels by Western blotting using its specific antibody.

unit/ml) and were represented as heat map and Venn diagram (Fig. 1, *A* and *B*). Gene ontology analysis shows the majority of these genes are involved in protein binding and catalytic activity (Fig. 1*C*). To validate the microarray data, we have studied the time-course effect of thrombin on the expression of 17 novel genes whose role in vascular wall remodeling is largely unknown (Fig. 1*D*). Among the genes tested, the expression of LMCD1 is highly induced by thrombin both at mRNA and pro-

tein levels (Fig. 1, *D* and *E*). To find the functional role of LMCD1, first we tested a longer time-course effect of thrombin on its expression in HASMCs. Thrombin induced LMCD1 expression in a sustained manner at both mRNA and protein levels (Fig. 2*A*). Second, we examined its role in HASMC apoptosis and proliferation. Thrombin had no effect on HASMC apoptosis as measured by TUNEL assay, and siRNA-mediated depletion of LMCD1 levels did not affect this cellular event (Fig. 2*B*, *top* and *middle panels*). On the other hand, thrombin-induced HASMC proliferation as measured by [^{3}H]thymidine incorporation and siRNA-mediated down-regulation of LMCD1 levels attenuated thrombin-induced HASMC DNA synthesis (Fig. 2*B*, *top* and *bottom panels*). These results indicate a role for LMCD1 in thrombin-induced HASMC replication. To explore the mechanisms by which LMCD1 mediates HASMC DNA synthesis, we first studied the time-course effect of thrombin on CDC6 and MCMs (MCM2-MCM7) that are involved in origin recognition complex (ORC) formation, an essential factor in the initiation of replication (15, 16). Thrombin induced CDC6 but not MCM levels in a sustained manner in HASMCs (Fig. 2*C*). In addition, silencing LMCD1 levels using its siRNA prevented thrombin-induced CDC6 expression, suggesting that LMCD1 plays a role in the regulation of CDC6 expression by thrombin in HASMCs (Fig. 2*D*). We also observed that depleting CDC6 levels by its siRNA blocks thrombin-induced DNA synthesis in HASMCs (Fig. 2*E*).

To understand the mechanisms by which LMCD1 mediates thrombin-induced CDC6 expression, we have cloned a ~1.2-kb human CDC6 promoter, and by TRANSFAC analysis we identified one nuclear factor of activated T cells (NFAT)-binding site at −473 nt and three E2F-binding sites at −279, −43, and −8 nt, respectively (Fig. 3*A*). In addition, cloning the 1.2-kb human CDC6 promoter into pGL3 basic vector and testing for its activity showed that thrombin induces CDC6 promoter activity by 3-fold, which is substantially attenuated by depletion of LMCD1 levels (Fig. 3*B*). To identify the minimal CDC6 promoter region required for thrombin-induced CDC6 promoter activity, we have subcloned the truncated regions −597 to +93 nt (0.690 kb), −354 to +93 nt (0.447 kb), −190 to +93 nt (0.283 kb), and −31 nt to +93 nt (0.124 kb) of CDC6 promoter into pGL3 basic vector, and the constructs were named as pGL3-CDC6p-(0.690 kb), pGL3-CDC6p-(0.447 kb), pGL3-CDC6p-(0.283 kb), and pGL3-CDC6p-(0.124 kb), respectively. We found that CDC6 promoter region from −190 to −31 nt of 0.283-kb promoter is sufficient for thrombin-induced CDC6 promoter activity (Fig. 3*C*). In addition, knockdown of LMCD1 levels by its siRNA prevented thrombin-induced CDC6 (0.283 kb) promoter activity (Fig. 3*D*). This result demonstrates that thrombin-induced LMCD1-responsive regulatory element(s) of CDC6 promoter is present within this 0.283-kb region. Because −190 to −31 nt of 0.283 kb promoter contains only one potential E2F-binding site at −43 nt, we mutated this site and tested its response to thrombin. Site-directed mutagenesis of E2F-binding site at −43 nt significantly reduced thrombin-induced CDC6 promoter activity (Fig. 3*E*), suggesting the importance of this E2F site in thrombin-induced CDC6 expression. Having found the requirement of this E2F site in thrombin-induced CDC6 promoter activity and that a role for E2Fs in the expression of CDC6 has been reported previously (17), we next sought to examine the role of E2Fs in thrombin-induced CDC6 expression. Toward this end, depletion of E2F1 by it siRNA blocked thrombin-induced CDC6 expression in HASMCs (Fig. 3*F*). This result infers that E2F1 is also essential for thrombin-induced CDC6 expression. Based on these observations, we wanted to explore any link between LMCD1 and E2F1 in CDC6 expression by thrombin. In this regard we measured DNA-binding activity by EMSA using the E2F-binding element at −43 nt as a biotin-labeled double-stranded oligonucleotide probe. Thrombin induced E2F DNA-binding activity in a time-dependent manner (Fig. 3*G*). In addition, supershift EMSA using anti-E2F1 or anti-LMCD1 antibodies showed the presence of both E2F1 and LMCD1 in thrombin-induced E2F DNA–protein complexes (Fig. 3*H*). To confirm the binding of E2F1 and LMCD1 to the E2F-binding site at −43 nt in the CDC6 promoter, we mutated this site in the oligonucleotide and used it as a probe for EMSA and supershift EMSA. In both EMSA and supershift EMSA, no DNA–protein complexes were formed with nuclear extracts of either control or thrombin-treated HASMCs using the mutant probe (Fig. 3*I*). The ChIP assay with anti-E2F1 and anti-LMCD1 antibodies demonstrates that E2F1 and LMCD1 bind to the same promoter region of CDC6 (Fig. 3*J*). Furthermore, the re-ChIP analysis of anti-LMCD1 chromatin immunocomplexes showed that E2F1 binds to the CDC6 promoter along with LMCD1. Likewise, re-ChIP analysis of anti-E2F1 chromatin immunocomplexes revealed that LMCD1 binds to CDC6 promoter along with E2F1 (Fig. 3*J*). These results imply that LMCD1 may interact with E2F1 in the transcriptional regulation of CDC6 by thrombin in HASMCs.

To determine whether LMCD1 physically interacts with E2F1 in mediating thrombin-induced CDC6 expression, we performed *in situ* proximal ligation assay (PLA), a powerful method to detect protein–protein interactions *in vivo* (18). The PLA results showed that LMCD1 interacts with E2F1 in response to thrombin at 4 h (Fig. 4*A*). This result indicates that LMCD1 interacts with E2F1 in response to thrombin in HASMCs. To identify the protein domains involved in their physical interaction, we next constructed the full-length and various truncations of LMCD1 and E2F1 in Myc-DDK-tagged and HA-tagged pCMV vectors, respectively (Fig. 4, *B* and *C*). When the full-length or various truncates of LMCD1 were co-expressed with the full-length of E2F1, we found that only PET–LIM1 domain but not Cys, PET, LIM1, or LIM2 domains alone or any of their other combinations were able to interact with E2F1 (Fig. 4*D*). Similarly, when the full-length or various truncations of HA-tagged E2F1 were co-expressed with full-length Myc-DDK-tagged LMCD1, in addition to its full length, only the mixed box domain (243–317 amino acids) of E2F1 interacts with LMCD1 (Fig. 4*E*). Furthermore, although the expression of E2F1 or LMCD1 alone induced the CDC6 promoter activity to some extent, co-expression of E2F1 along with LMCD1 or its PET–LIM1 domain but not PET–LIM2 domain further enhanced the CDC6 promoter activity (Fig. 4*F*). To further confirm the interdependence between E2F1 and LMCD1 on CDC6 promoter activity, we overexpressed E2F1 or LMCD1 in the absence of LMCD1 or E2F1, respectively, and measured

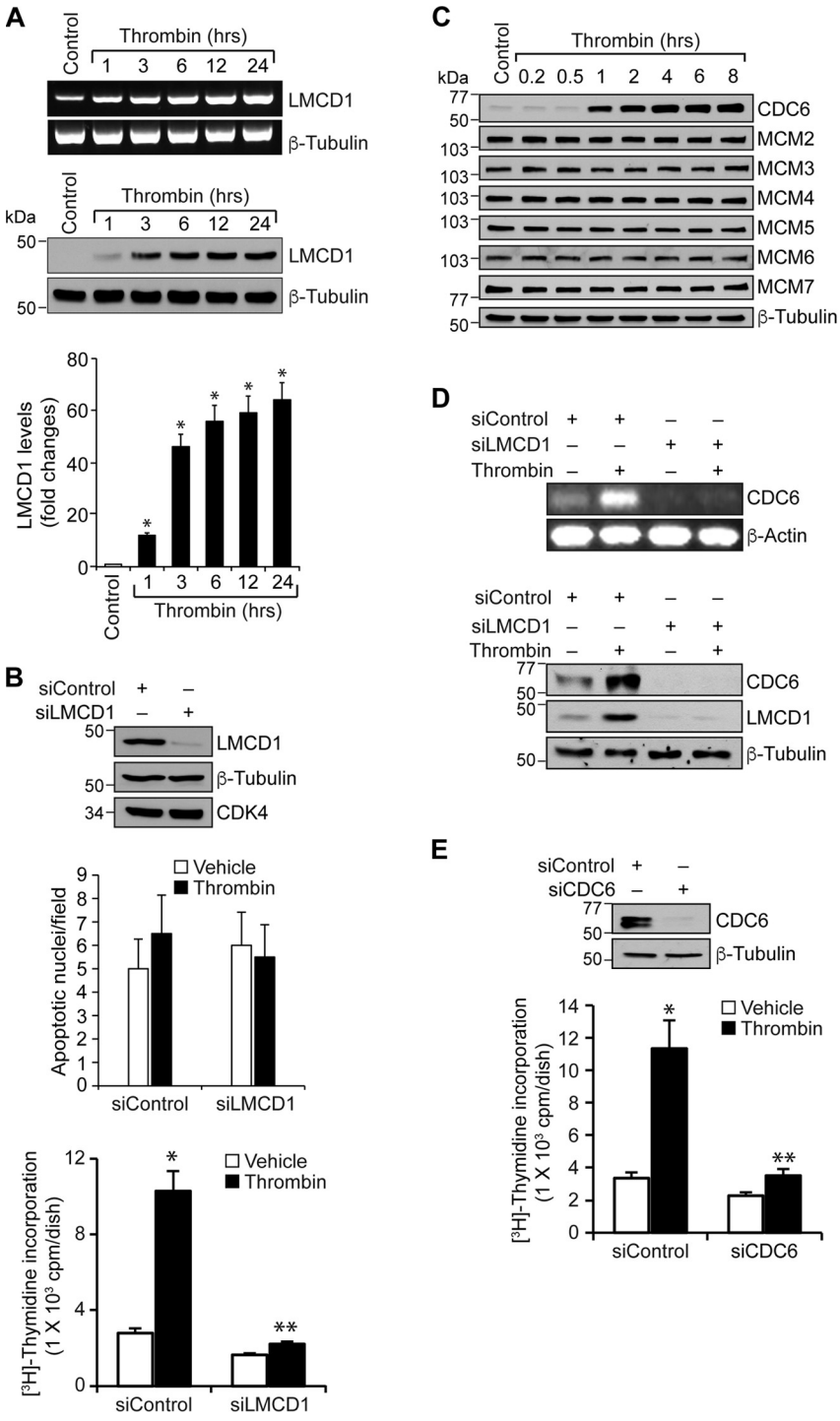

Figure 2. LMCD1 plays a role in thrombin-induced CDC6 expression and DNA synthesis in HASMCs. *A*, growth-arrested HASMCs were treated with and without thrombin (0.5 unit/ml) for the indicated time periods, and either RNA was isolated and analyzed by RT-PCR for LMCD1 mRNA levels using its specific primers, or cell extracts were prepared and analyzed by Western blotting for LMCD1 protein levels using its specific antibodies. *B*, *top panel*, HASMCs were transfected with siControl or siLMCD1 (100 nM). For 48 h later, cell extracts were prepared and analyzed by Western blotting for LMCD1 levels using its specific antibody, and the blot was normalized to β-tubulin and CDK4 levels. *Middle* and *bottom panels*, HASMCs that were transfected with siControl or siLMCD1 and growth-arrested were treated with vehicle or thrombin (0.5 unit/ml) for 36 h, apoptosis was measured by TUNEL assay (*middle panel*), and DNA synthesis was measured by [^{3}H]thymidine incorporation (*bottom panel*). *C*, equal amounts of protein from control and various time periods of thrombin-treated HASMCs were analyzed by Western blotting for CDC6 and MCM2–7 levels using their specific antibodies, and the CDC6 blot was normalized to β-tubulin. *D*, HASMCs that were transfected with the indicated siRNA were treated with and without thrombin for 2 h, and either RNA was isolated, or cell extracts were prepared and analyzed by RT-PCR and Western blotting, respectively, for CDC6 mRNA and protein levels using its specific primers or antibodies and normalized to β-actin transcripts or β-tubulin levels, respectively. *E*, *upper panel*, HASMCs were transfected with siControl or siCDC6 (100 nM), and 48 h later cell extracts were prepared and analyzed by Western blotting for CDC6 levels, and the blot was normalized to β-tubulin. *Lower panel*, HASMCs that were transfected with siControl or siCDC6 and growth-arrested were treated with and without thrombin (0.5 unit/ml) for 36 h, and DNA synthesis was measured by [^{3}H]thymidine incorporation. *, $p < 0.05$ *versus* control or siControl; **, $p < 0.05$ *versus* siControl + thrombin.

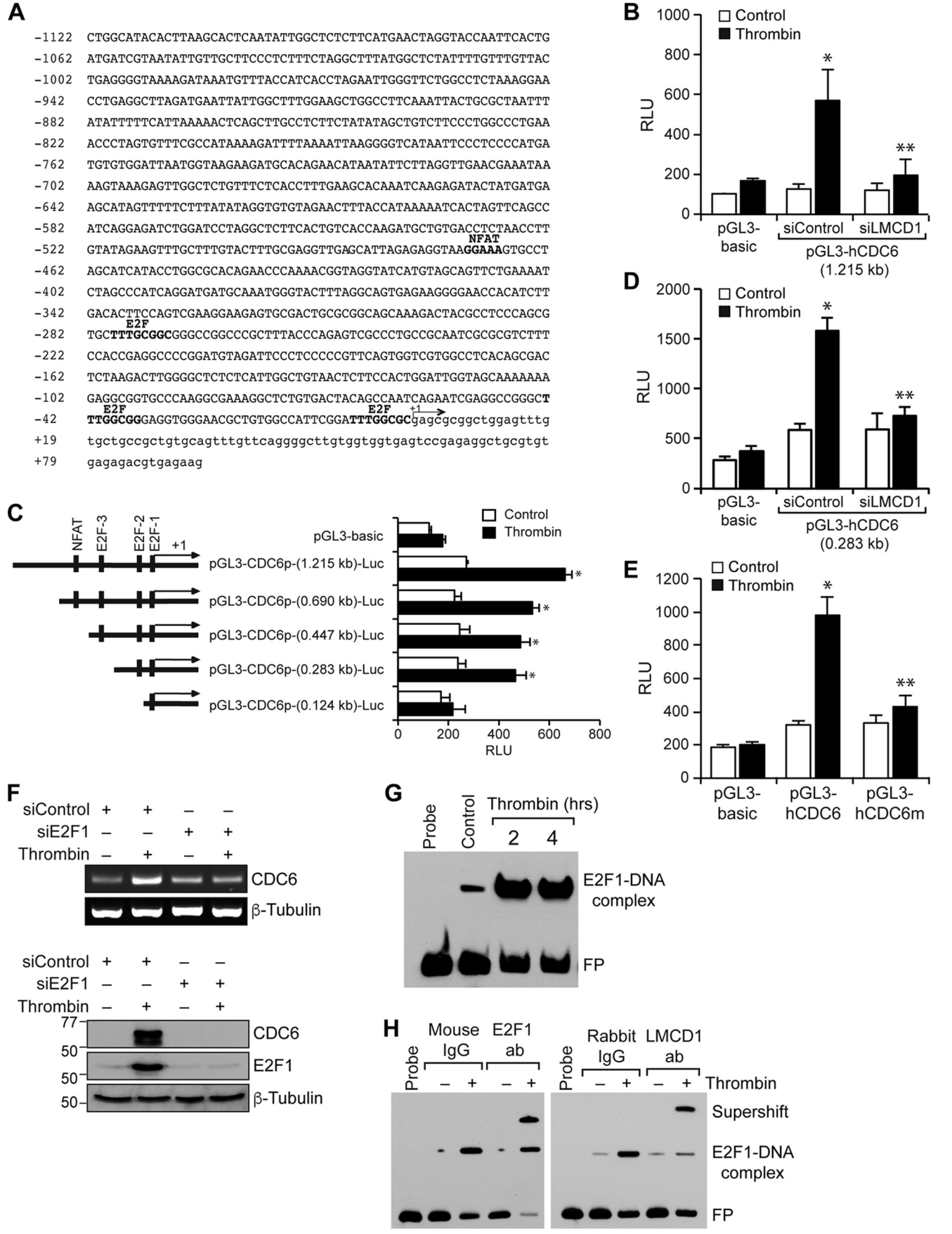
A
-1122 CTGGCATACACTTAAGCACTCAATATTGGCTCTCTTCATGAACTAGGTACCAATTCACTG
-1062 ATGATCGTAATATTGTTGCTTCCCTCTTTCTAGGCTTTATGGCTCTATTTTGTTTGTTAC
-1002 TGAGGGGTAAAAGATAAATGTTTACCATCACCTAGAATTGGGTTCTGGCCTCTAAAGGAA
-942 CCTGAGGCTTAGATGAATTATTGGCTTTGGAAGCTGGCCTTCAAATTACTGCGCTAATTT
-882 ATATTTTTCATTAAAAACTCAGCTTGCCTCTTCTATATAGCTGTCTTCCCTGGCCCTGAA
-822 ACCCTAGTGTTTCGCCATAAAAGATTTTAAAATTAAGGGGTCATAATTCCCTCCCCATGA
-762 TGTGTGGATTAATGGTAAGAAGATGCACAGAACATAATATTCTTAGGTTGAACGAAATAA
-702 AAGTAAAGAGTTGGCTCTGTTTCTCACCTTTGAAGCACAAATCAAGAGATACTATGATGA
-642 AGCATAGTTTTTCTTTATATAGGTGTGTAGAACTTTACCATAAAAATCACTAGTTCAGCC
-582 ATCAGGAGATCTGGATCCTAGGCTCTTCACTGTCACCAAGATGCTGTGACCTCTAACCTT
-522 GTATAGAAGTTTGCTTTGTACTTTGCGAGGTTGAGCATTAGAGAGGTAAGGAAAGTGCCT
-462 AGCATCATACCTGGCGCACAGAACCCAAAACGGTAGGTATCATGTAGCAGTTCTGAAAAT
-402 CTAGCCCATCAGGATGATGCAAATGGGTACTTTAGGCAGTGAGAAGGGGAACCACATCTT
-342 GACACTTCCAGTCGAAGGAAGAGTGCGACTGCGCGGCAGCAAAGACTACGCCTCCCAGCG
-282 TGCTTTGCGGCGGGCCGGCCCGCTTTACCCAGAGTCGCCCTGCCGCAATCGCGCGTCTTT
-222 CCACCGAGGCCCCGGATGTAGATTCCCTCCCCCGTTCAGTGGTCGTGGCCTCACAGCGAC
-162 TCTAAGACTTGGGGCTCTCTCATTGGCTGTAACTCTTCCACTGGATTGGTAGCAAAAAAA
-102 GAGGCGGTGCCCAAGGCGAAAGGCTCTGTGACTACAGCCAATCAGAATCGAGGCCGGGCT
-42 TTGGCGGGAGGTGGGAACGCTGTGGCCATTCGGATTTGGCGCgagcgcggctggagtttg
+19 tgctgccgctgtgcagtttgttcaggggcttgtggtggtgagtccgagaggctgcgtgt
+79 gagagacgtgagaag
E2F
E2F
E2F
NFAT
B
Control
Thrombin
RLU
pGL3-basic
siControl
siLMCD1
pGL3-hCDC6 (1.215 kb)
C
NFAT
E2F-3
E2F-2
E2F-1
+1
pGL3-basic
pGL3-CDC6p-(1.215 kb)-Luc
pGL3-CDC6p-(0.690 kb)-Luc
pGL3-CDC6p-(0.447 kb)-Luc
pGL3-CDC6p-(0.283 kb)-Luc
pGL3-CDC6p-(0.124 kb)-Luc
RLU
D
pGL3-hCDC6 (0.283 kb)
E
pGL3-hCDC6
pGL3-hCDC6m
F
siControl
siE2F1
Thrombin
CDC6
β-Tubulin
E2F1
G
Probe
Control
Thrombin (hrs)
2
4
E2F1-DNA complex
FP
H
Mouse IgG
E2F1 ab
Rabbit IgG
LMCD1 ab
Supershift

the CDC6 promoter activity. Overexpression of either LMCD1 in the absence of E2F1 or E2F1 in the absence of LMCD1 did not result in enhanced CDC6 promoter activity (Fig. 4*G*). On the other hand, co-expression of E2F1 with LMCD1 or its PET–LIM1-LIM2 or PET–LIM1 but not PET–LIM2 domain increased CDC6 expression at protein levels (Fig. 4*H*), suggesting that LMCD1 via its PET–LIM1 domains interacts with E2F1 to enhance CDC6 expression in HASMCs.

To elucidate the upstream signaling mechanisms of thrombin-induced LMCD1-mediated CDC6 expression, we have tested the role of protease-activated receptor 1 (PAR1) and its downstream G proteins using pharmacological and siRNA approaches, respectively. SCH79797, the specific antagonist of PAR1 (19), substantially reduced thrombin-induced LMCD1 and CDC6 expression, CDC6 promoter activity, and DNA synthesis in HASMCs (Fig. 5, *A–D*). In addition, thrombin caused a time-dependent dissociation of $G\alpha_{q/11}$ but not $G\alpha_{12}$ or $G\alpha_{13}$ from PAR1 in response to thrombin (Fig. 5*E*), suggesting that thrombin activates $G\alpha_{q/11}$ downstream to PAR1 in HASMCs. Furthermore, silencing $G\alpha_{q/11}$ using their siRNAs prevented thrombin-induced LMCD1 and CDC6 expression, CDC6 promoter activity, and DNA synthesis in HASMCs (Fig. 5, *F–J*). Several studies suggest that GPCR agonists stimulate PLCβs in facilitating their cellular effects (20, 21). To test the role of PLCβs in thrombin-induced LMCD1/E2F1-CDC6 signaling, we first studied the time-course effect of thrombin on the steady-state levels of PLCβ isoforms. Thrombin had no effect on PLCβ1–3 levels, and the presence of PLCβ4 was not detected in HASMCs (Fig. 6*A*). Next, using the fluorogenic PLC substrate WH-15 (22), we studied the effect of thrombin on their activities. Thrombin induced PLCβ3 but not PLCβ1 or PLCβ2 activities in a time-dependent manner in HASMCs (Fig. 6*B*). To find whether PAR1 and $G\alpha_{q/11}$ activation is required for thrombin-induced PLCβ3 activity, we tested the effect of SCH79797 and si$G\alpha_{q/11}$ on PLCβ3 activity. Inhibition of PAR1 by its antagonist SCH79797 or depletion of $G\alpha_{q/11}$ levels by their siRNAs blocked thrombin-induced PLCβ3 activity (Fig. 6, *C* and *D*). Furthermore, depletion of PLCβ3 levels by its short-hairpin RNA expression plasmid (23) inhibited thrombin-induced LMCD1 and CDC6 expression, CDC6 promoter activity,

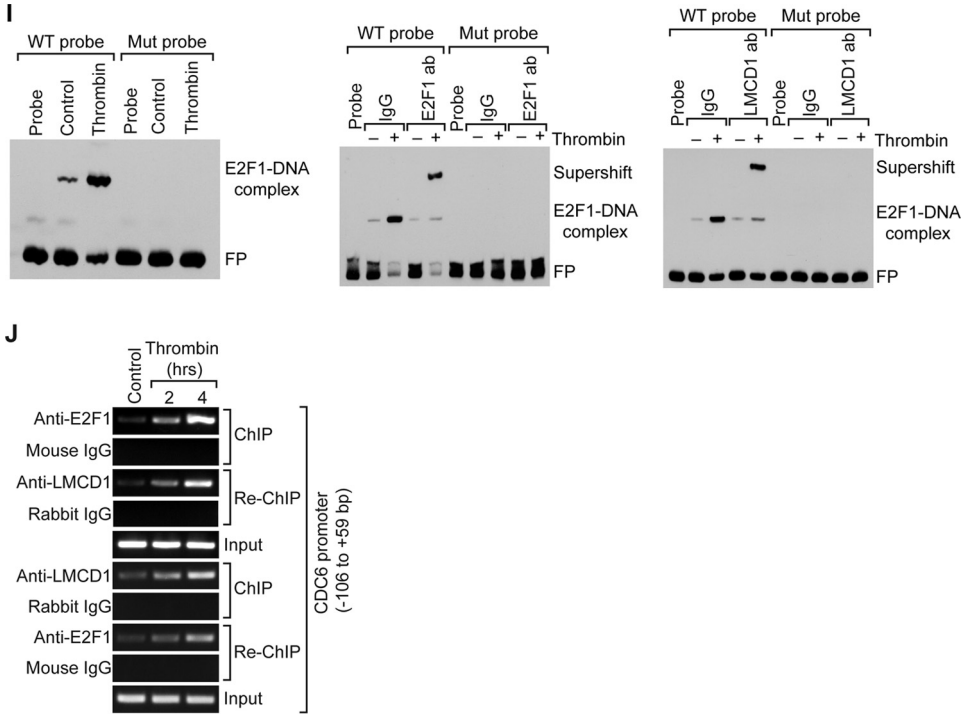

Figure 3—*continued*

Figure 3. LMCD1 acts as a co-activator for E2F1 in mediating thrombin-induced CDC6 promoter activity. *A*, CDC6 promoter encompassing from −1122 to +93 nt (1.215 kb) was cloned into pGL3-basic vector and sequenced. *B*, HASMCs were transfected with pGL3-basic vector or pGL3-CDC6 promoter (1.215 kb) in combination with siControl or siLMCD1, growth-arrested, and treated with and without thrombin (0.5 unit/ml) for 6 h, and the luciferase activities were measured. *C*, HASMCs that were transfected with pGL3-basic vector or pGL3-CDC6 promoter reporter gene constructs with serial 5′-deletions were quiesced and treated with and without thrombin (0.5 unit/ml) for 6 h and analyzed for luciferase activity. *D*, HASMCs were transfected with pGL3-basic vector or pGL3-CDC6 promoter (0.283 kb) in combination with siControl or siLMCD1, growth-arrested, and treated with and without thrombin (0.5 unit/ml) for 6 h, and the luciferase activities were measured. *E*, HASMCs were transfected with pGL3-basic vector or pGL3-hCDC6 promoter with and without the mutated E2F-binding site (at −43 nt), quiesced, and treated with and without thrombin for 6 h, and the luciferase activity was measured. *F*, HASMCs that were transfected with siControl or siE2F1 and growth-arrested were treated with and without thrombin (0.5 unit/ml) for 6 h, and either RNA was isolated, or cell extracts were prepared analyzed by RT-PCR and Western blotting, respectively, for CDC6 mRNA and protein levels using its specific primers or antibodies and normalized to β-actin transcripts or β-tubulin levels, respectively. *G*, nuclear extracts of control and various time periods of thrombin-treated HASMCs were analyzed by EMSA using the E2F-binding element at −43 nt as a biotin-labeled probe. *H*, nuclear extracts of control and 4 h of thrombin-treated cells were analyzed for the presence of E2F1 and LMCD1 in the E2F–DNA complexes by supershift EMSA. *I*, all the conditions were same as in *H*, except that both WT and mutant (*Mut*) probes were used. *J*, quiescent HASMCs were treated with and without thrombin for the indicated time periods and subjected to ChIP and re-ChIP assays for CDC6 promoter region encompassing the E2F site at −43 nt using anti-E2F1 or anti-LMCD1 antibodies with the indicated sequential order. *, $p < 0.05$ *versus* control or siControl; **, $p < 0.05$ *versus* thrombin or siControl + thrombin. *RLU*, relative luciferase units. *FP*, free probe.

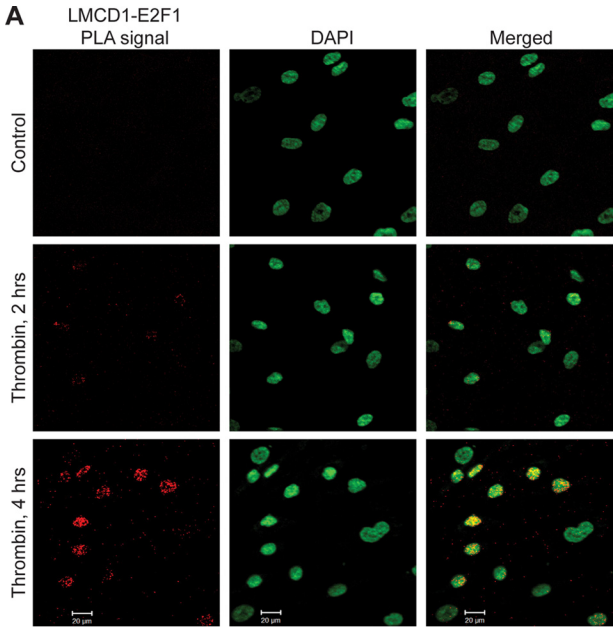

Figure 4. LMCD1 interacts with E2F1 in mediating thrombin-induced CDC6 promoter activity. *A*, quiescent HASMCs were treated with or without thrombin for the indicated time periods, fixed, and incubated with mouse anti-E2F1 and rabbit anti-LMCD1 antibodies. After washing, the cells were incubated with anti-mouse PLUS oligonucleotides and anti-rabbit MINUS oligonucleotide-conjugated secondary antibodies. The protein interactions were observed under confocal microscope using 20× magnification. *B* and *C*, the cloning strategy for full-length and various truncations of LMCD1 and E2F1 in Myc-DDK-tagged and HA-tagged pCMV expression vectors. *D*, Myc-DDK-tagged full-length or various truncations of LMCD1 were co-transfected with HA-tagged full-length E2F1 in HASMCs, and 36 h later cell extracts were prepared, immunoprecipitated with the indicated antibodies, and immunoblotted with the indicated antibodies. *E*, HA-tagged full-length or various truncations of E2F1 co-transfected with Myc-DDK-tagged full LMCD1 in HASMCs, and 36 h later cell extracts were prepared, immunoprecipitated with the indicated antibodies, and immunoblotted with the indicated antibodies. *F*, the pGL3-basic vector and the pGL3-hCDC6 promoter were co-transfected with E2F1, LMCD1, or various truncations of LMCD1 in HASMCs, and 36 h later cell extracts were prepared and analyzed for luciferase activity. *G*, the pGL3-basic vector and the pGL3-hCDC6 promoter were co-transfected with the indicated siRNA in the presence and absence of pCMV-LMCD1 or pCMV-E2F1 constructs in HASMCs, and 36 h later cell extracts were prepared and assayed for luciferase activity. *H*, Myc-DDK-tagged full-length or various truncations of LMCD1 were co-transfected with HA-tagged full-length E2F1 in HASMCs, and 36 h later cell extracts were prepared analyzed by Western blotting for CDC6 levels and normalized with β-tubulin. *, $p < 0.05$ *versus* pCMV-EV or siControl; **, $p < 0.05$ *versus* pCMV-LMCD1, pCMV-E2F1 or siControl + pCMV-LMCD1. *DAPI*, 4′,6′-diamino-2-phenylindole; *IB*, immunoblot; *IP*, immunoprecipitation.

and DNA synthesis in HASMCs (Fig. 6, *E–H*). These observations imply that PLCβ3 plays an important role in LMCD1/E2F1-mediated CDC6 expression promoting DNA synthesis in HASMC downstream to PAR1 and $G\alpha_{q/11}$.

To understand the role of LMCD1 in the modulation of VSMC proliferation *in vivo*, we used both mouse carotid artery ligation and rat carotid artery balloon injury as models for restenosis. Either ligation of mouse carotid artery or BI of rat carotid artery while inducing the expression of E2F1 and CDC6 decreased the LMCD1 expression (Fig. 7*A*). Thrombin also had no effect or decreased LMCD1 expression in MASMCs or RASMCs and down-regulation of LMCD1 levels, whereas attenuating DNA synthesis in HASMCs did not affect the DNA synthesis in MASMCs or RASMCs in response to thrombin (Fig. 7, *B* and *C*). To find whether LMCD1 plays a role in VSMC replication in a species and agonist-specific manner, we examined its involvement in PDGF-BB-induced VSMC DNA synthesis. Down-regulation of LMCD1 while attenuating PDGF-BB-induced DNA synthesis in HASMCs had no effect on MASMC or RASMC DNA synthesis (Fig. 7*D*). These observations clearly demonstrate that LMCD1 mediates VSMC DNA synthesis in a species-specific manner. Because LMCD1 was only involved in HASMC DNA synthesis and because of a lack of access to human restenosis artery tissue samples, we used human normal and atherosclerotic coronary artery samples as an *in vivo* model, because VSMC proliferation is a common phenomenon in both restenosis and during early development of atherosclerosis (24–28). It was interesting to note that LMCD1 expression was induced highly in SMC and co-localized with the cell proliferation marker Ki67 in human atherosclerotic lesions as compared with normal artery (Fig. 7*E*). Similarly, we found increased CDC6 expression in SMC, and it was co-localized with LMCD1 in human atherosclerotic lesions as compared with normal artery (Fig. 7*E*). Furthermore, LMCD1 expression was found to be co-localized with filipin staining in human atherosclerotic lesions as compared with normal artery (Fig. 7*E*). These findings reveal that LMCD1 via CDC6 expression, thereby promoting VSMC replication, might be involved in vascular pathologies such as restenosis and atherosclerosis.

Discussion

Increased vascular smooth muscle cell proliferation is a major contributing factor in restenosis following angioplasty (1–3). Many molecules produced at the site of vascular injury such as PDGF-BB, fibroblast growth factor 2, monocyte chemoattractant protein 1 (MCP1), and thrombin can influence the growth of VSMCs (7, 8, 29–31). Toward exploring the mechanisms of VSMC multiplication during restenosis, we found that thrombin induces the expression of LMCD1 in HASMCs. Previous studies have shown that LMCD1 represses transcriptional factor GATA6 and promotes cardiac hypertro-

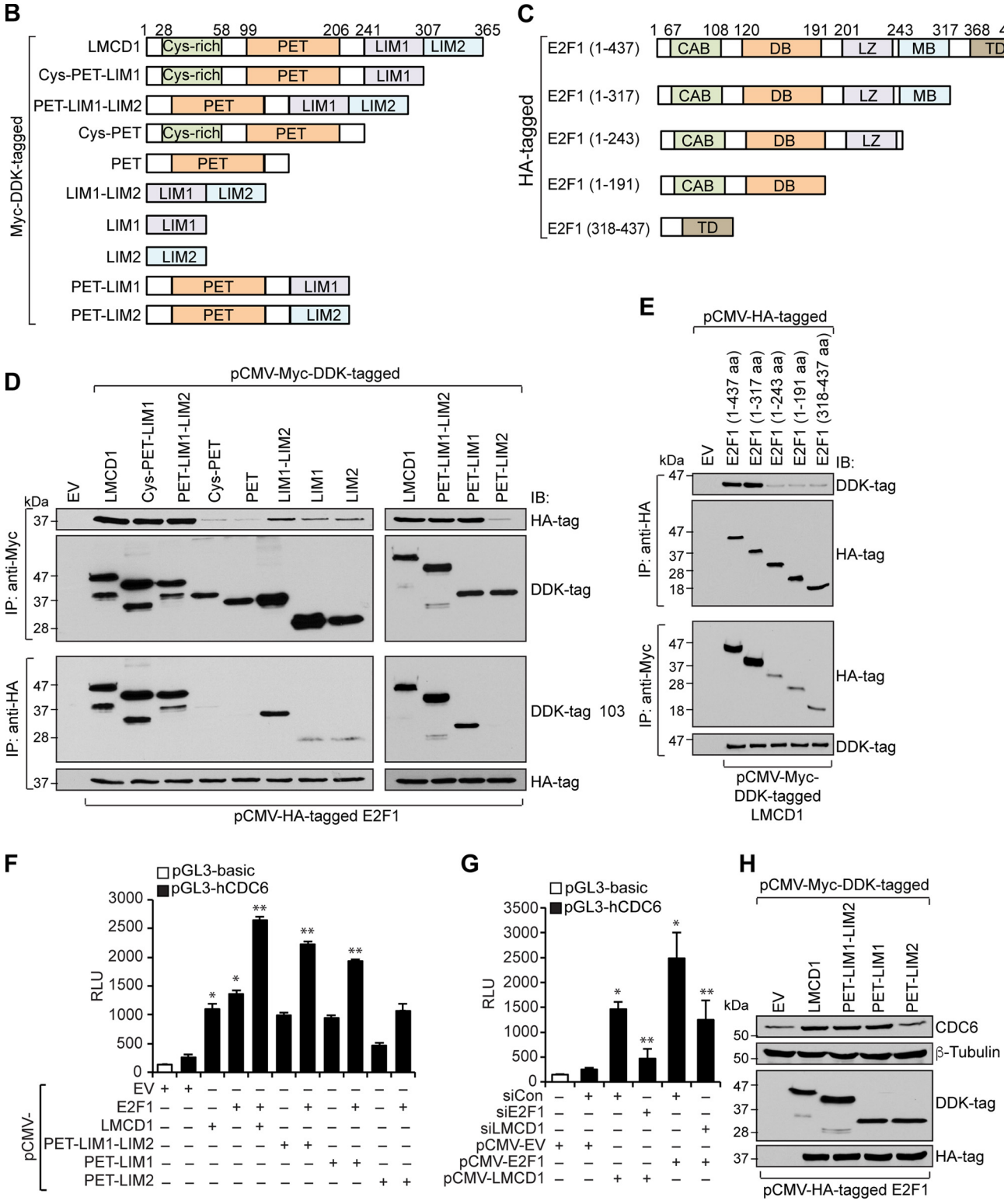

Figure 4—*continued*

phy (11, 12). In line with its role in cardiac hypertrophy, the present findings show that LMCD1 expression is required for thrombin-induced HASMC replication. Because it was reported to act as a repressor for GATA6 in promoting cardiac hypertrophy, we were intrigued to explore the mechanisms of its involvement in HASMC replication. Our findings show that LMCD1 is required for thrombin induction of CDC6 that plays a rate-limiting role in ORC formation during replication (15, 16). These observations suggest that through CDC6 expression, LMCD1 may play a role in the regulation of ORC formation during thrombin-induced VSMC proliferation. The promoter reporter gene analysis reveals the presence of throm-

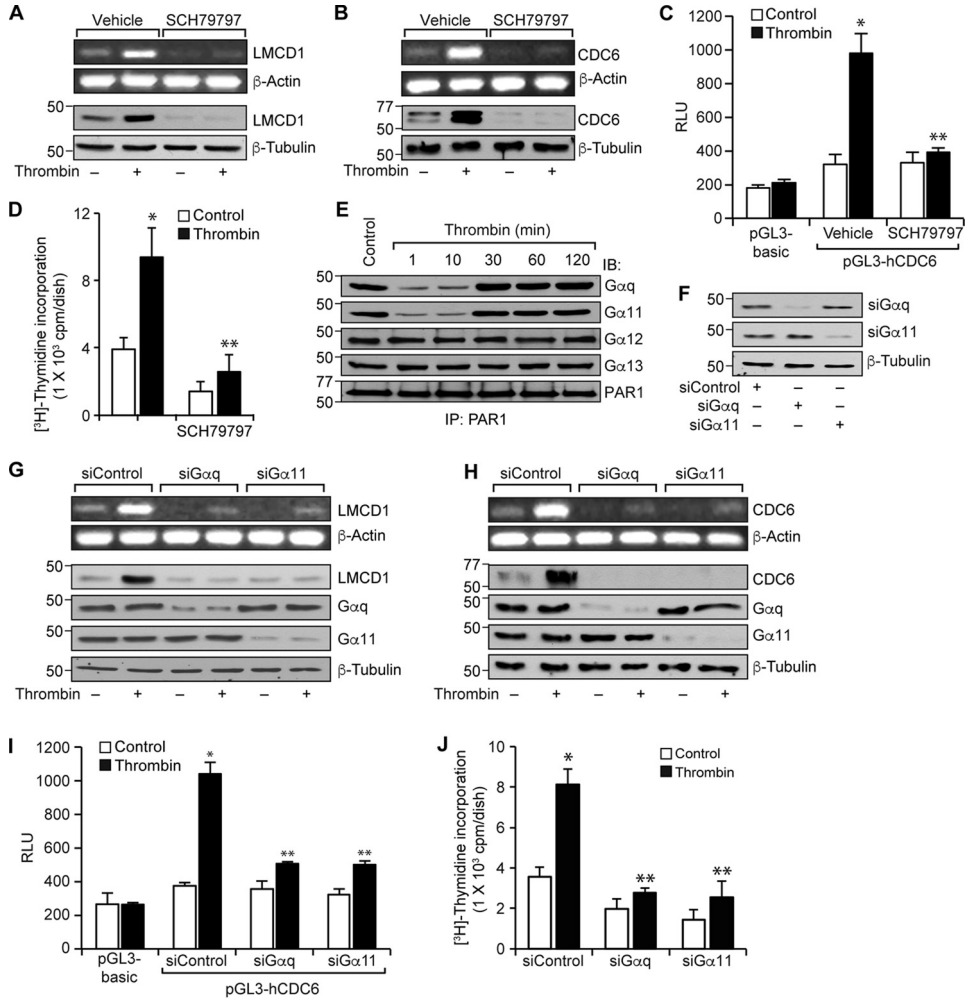

Figure 5. Par1 and $G\alpha_{q/11}$ mediate thrombin-induced LMCD1 and CDC6 expression in HASMCs. *A* and *B*, quiescent HASMCs were treated with and without thrombin (0.5 unit/ml) in the presence and absence of SCH79797 (10 μM), the Par1 antagonist, for 4 h, and either RNA was isolated or cell extracts were prepared analyzed by RT-PCR and Western blotting, respectively, for LMCD1 and CDC6 mRNA and protein levels using their specific primers or antibodies and normalized to β-actin transcripts or β-tubulin levels, respectively. *C*, the pGL3-basic vector and the pGL3-CDC6 promoter were transfected in HASMCs, growth-arrested, and treated with vehicle or thrombin (0.5 unit/ml) in the presence of SCH79797 for 6 h, and the luciferase activities were measured. *D*, quiescent HASMCs were treated with and without thrombin (0.5 unit/ml) in the presence and absence of SCH79797 for 36 h, and DNA synthesis was measured by [^{3}H]thymidine incorporation. *E*, cell extracts of control and various time periods of thrombin (0.5 unit/ml)-treated HASMCS were immunoprecipitated with anti-Par1 antibodies, and the immunocomplexes were analyzed by Western blotting for the indicated Gα proteins using their specific antibodies and normalized to Par1 levels. *F*, HASMCs were transfected with siControl, si$G\alpha_q$, or si$G\alpha_{11}$, and 36 h later the cell extracts were prepared and analyzed by Western blotting for $G\alpha_q$, $G\alpha_{11}$, or β-tubulin levels using their specific antibodies. *G* and *H*, HASMCs that were transfected with siControl, si$G\alpha_q$, or si$G\alpha_{11}$ and growth-arrested were treated with and without thrombin (0.5 unit/ml) for 4 h, and either total cellular RNA was isolated, or cell extracts were prepared analyzed by RT-PCR and Western blotting, respectively, for LMCDI and CDC6 mRNA and protein levels using their specific primers or antibodies and normalized to β-actin transcripts or β-tubulin levels, respectively. The LMCDI and CDC6 blots were reprobed for $G\alpha_q$, $G\alpha_{11}$, or β-tubulin levels to show the efficacy of the siRNA on its target and off target molecule levels. *I*, HASMCs were transfected with pGL3-basic vector or pGL3-CDC6 promoter in combination with siControl, si$G\alpha_q$, or si$G\alpha_{11}$, growth-arrested, and treated with and without thrombin (0.5 unit/ml) for 6 h, and cell extracts were prepared and analyzed for luciferase activity. *J*, all the conditions were the same as in *G* except that cells were subjected to thrombin (0.5 unit/ml)-induced DNA synthesis using [^{3}H]thymidine incorporation. *, $p <$ 0.05 *versus* control or siControl; **, $p < 0.05$ *versus* thrombin or siControl + thrombin. *RLU*, relative luciferase units.

bin-responsive element in CDC6 promoter within a 300-bp region from the transcription start site. Because this region contains three E2F-binding sites and because site-directed mutagenesis shows that the E2F binding site at −43 nt is essential for thrombin-induced CDC6 promoter activity, it is implied that LMCD1-mediated CDC6 expression also depends on this regulatory element. Because the down-regulation of E2F1 levels also abolished thrombin-induced CDC6 promoter activity, it is likely that LMCD1 interacts with E2F1 in the regulation of CDC6 expression. This view can be supported by the observations that both LMCD1 and E2F1 bind to a E2F-binding site as demonstrated by EMSA, supershift EMSA, ChIP, and re-ChIP assays. In fact, the PLA findings reveal that LMCD1 physically interacts with E2F1 in response to thrombin in HASMCs. Furthermore, the protein–protein interaction studies show that LMCD1 interacts with E2F1 via involving its PET–LIM1 domains. It was shown that E2Fs modulate their target gene expression via interacting with their co-activators (32). In this context, it was shown that ACTR acts as a co-activator for E2F in the regulation of a subset of genes (32). In co-transfection experiments, we found that although expression of LMCD1 or E2F1 alone exhibited CDC6 promoter activity to some extent, when both were simultaneously transfected, the CDC6 promoter activity was enhanced. In addition, LMCD1 PET–LIM1

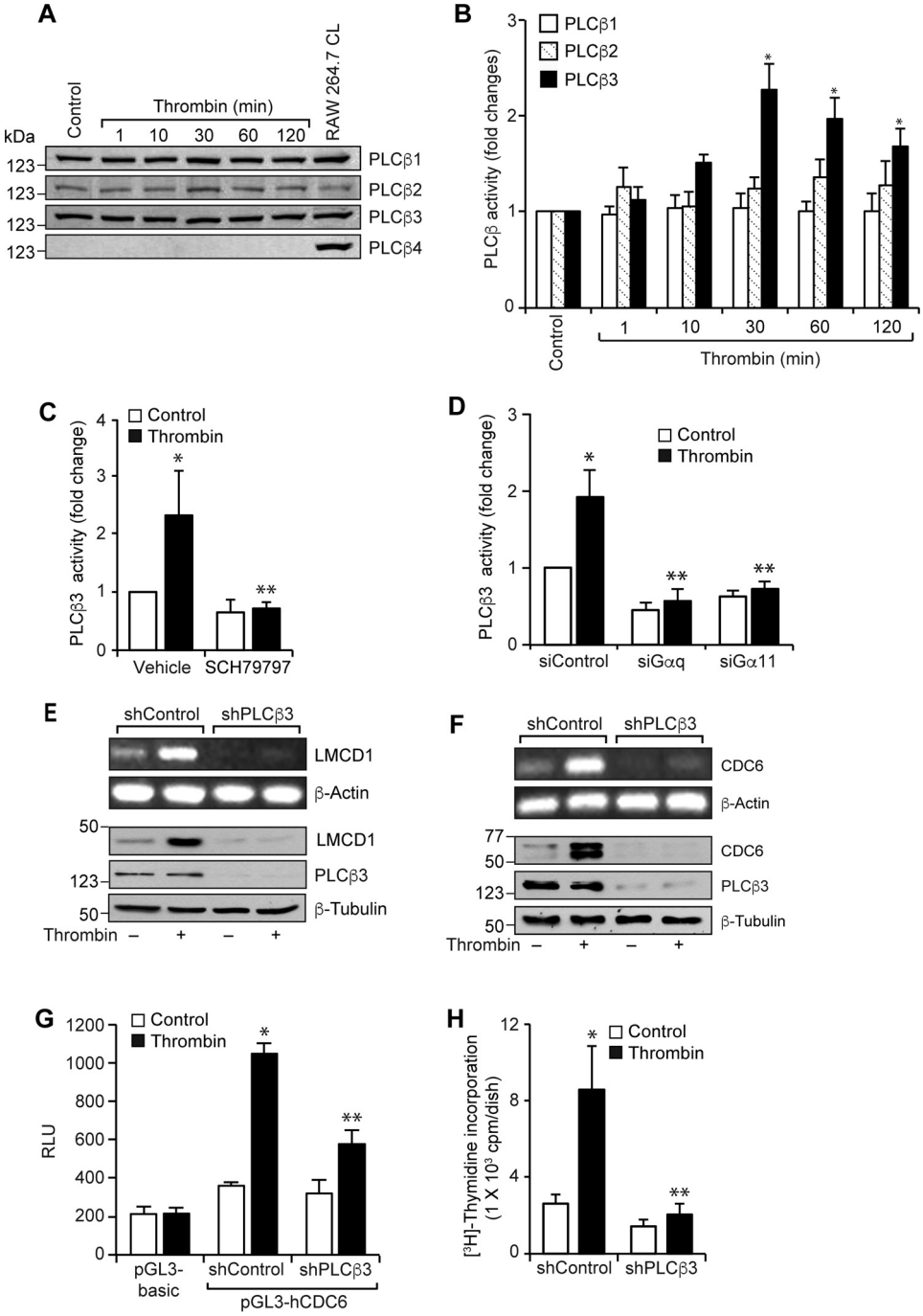

Figure 6. PLCβ3 mediates thrombin-induced LMCDI and CDC6 expression. *A* and *B*, cell extracts of control and various time periods of thrombin (0.5 unit/ml)-treated HASMCs were analyzed by Western blotting for PLCβ1–4 levels using their specific antibodies and normalized to β-tubulin (*A*) or immunoprecipitated with anti-PLCβ1–3 antibodies, and their activities were measured using a fluorogenic PLC substrate, WH-15 (*B*). *C*, quiescent HASMCs were treated with and without thrombin in the presence and absence of SCH79797 for 30 min and assayed for PLCβ3 activity. *D*, HASMCs that were transfected with siControl, siGα_q, or siGα_{11} and quiesced were treated with and without thrombin for 30 min and PLCβ3 activity was measured. *E* and *F*, cells were transfected with shControl or shPLCβ3 plasmid, growth-arrested, and treated with and without thrombin (0.5 unit/ml) for 4 h, and either total cellular RNA was isolated, or cell extracts were prepared and analyzed by RT-PCR and Western blotting, respectively, for LMCDI and CDC6 mRNA and protein levels using their specific primers or antibodies and normalized to β-actin transcripts or β-tubulin levels, respectively. The LMCD1 blot was reprobed for PLCβ3 or β-tubulin to show the efficacy and specificity of the short-hairpin RNA on it target and off target molecules. *G*, HASMCs were transfected with pGL3-basic vector or pGL3-CDC6 promoter in combination with shControl or shPLCβ3 plasmid, growth-arrested, and treated with and without thrombin (0.5 unit/ml) for 6 h, and cell extracts were prepared and assayed for luciferase activity. *H*, HASMCs were transfected with shControl or shPLCβ3, growth-arrested, and treated with and without thrombin (0.5 unit/ml) for 36 h, and DNA synthesis was measured by [^{3}H]thymidine incorporation. *, $p < 0.05$ *versus* control or siControl; **, $p < 0.05$ *versus* thrombin or siControl + thrombin. *RLU*, relative luciferase units.

domains were found to be sufficient to enhance the E2F1-mediated CDC6 promoter activity, which is consistent with its binding capacity with E2F1. In addition, when cellular E2F1 levels were depleted, overexpression of LMCD1 had no effect on CDC6 promoter activity. Similarly, when cellular LMCD1 levels were depleted, overexpression of E2F1 resulted only in a

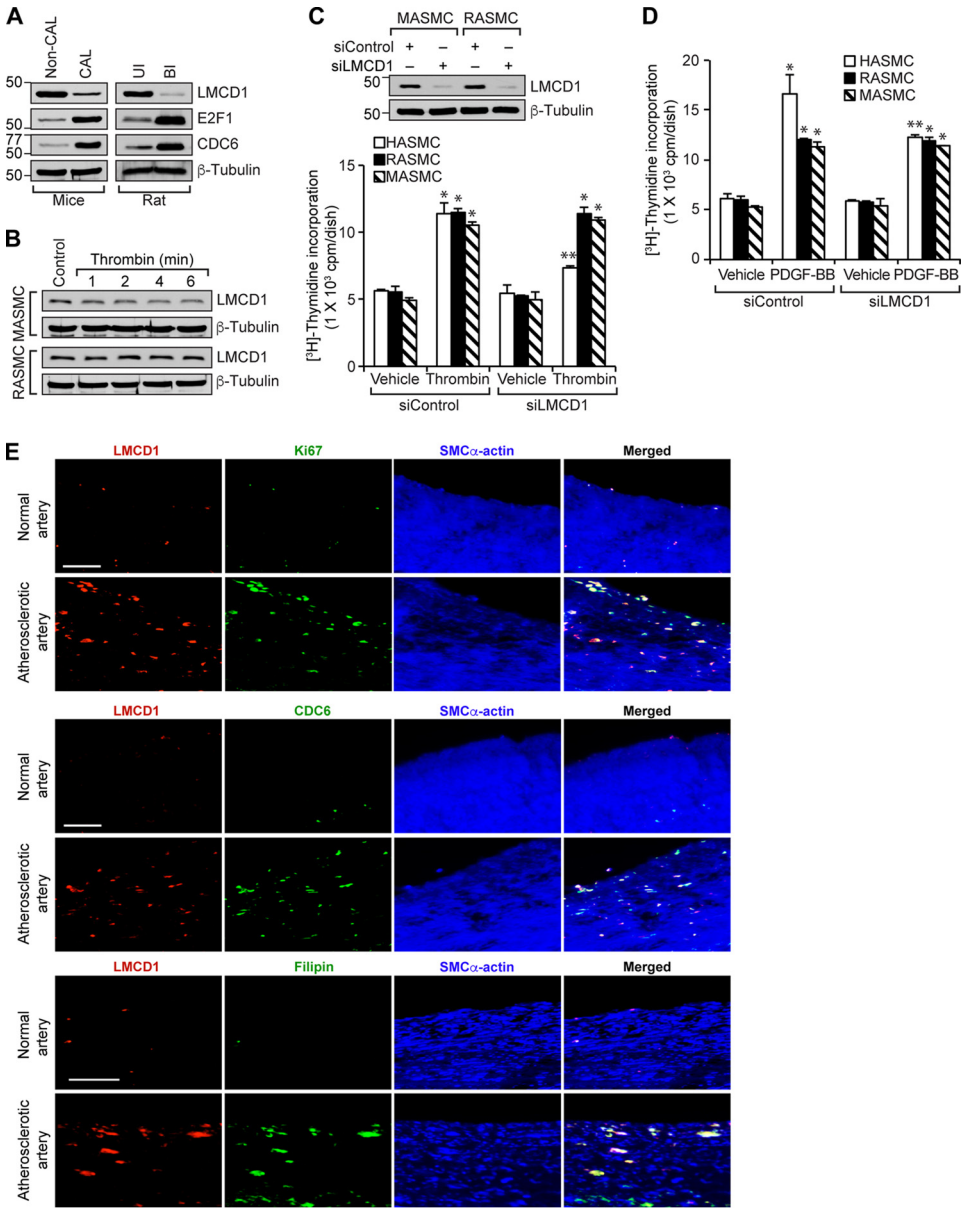

Figure 7. The lack of a role of LMCD1 in mouse or rat aortic smooth muscle cell proliferation. *A*, tissue extracts were prepared from control and ligated mice carotid arteries, and uninjured (*UI*) and balloon-injured rat carotid arteries were analyzed by Western blotting for LMCD1, E2F1, and CDC6 levels using their specific antibodies and normalized to β-tubulin levels. *B*, quiescent MASMCs and RASMCs were treated with and without thrombin (0.5 unit/ml) for the indicated time periods and analyzed by Western blotting for LMCD1 levels and normalized to β-tubulin. *C*, *upper panel*, MASMCs and RASMCs were transfected with siControl or siLMCD1 for 36 h and analyzed by Western blotting for LMCD1 levels and normalized to β-tubulin. *Lower panel*, HASMCs, MASMCs, and RASMCs were transfected with siControl or siLMCD1, growth-arrested, and treated with and without thrombin (0.5 unit/ml), and DNA synthesis was measured by [^{3}H]thymidine incorporation. *D*, all the conditions were same as in the *bottom panel* of *C* except that cells were treated with and without PDGF-BB and DNA synthesis was measured by [^{3}H]thymidine incorporation. *E*, paraffin-embedded human normal and atherosclerotic artery sections were stained for LMCD1 (*red*) and SMCα-actin (*blue*) in combination with Ki67 (*green*), CDC6 (*green*), or filipin (*green*). *Scale bar*, 50 μm. *, $p < 0.05$ *versus* siControl; **, $p < 0.05$ *versus* siControl + thrombin.

small increase in CDC6 promoter activity. These results collectively infer that LMCD1 acts as a co-activator for E2F1 in thrombin-induced CDC6 expression mediating HASMC replication.

In regard to the upstream signaling, our results show that Par1-dependent $G\alpha_{q/11}$ activation is involved in thrombin-induced LMCD1 and CDC6 expression and DNA synthesis. The role of PAR1 and $G\alpha_{q/11}$ in the regulation of VSMC growth has been reported previously (33, 34). Similarly, the involvement of PLCβ in the regulation of VSMC growth has also been demonstrated (20, 33). The findings that thrombin activates PLCβ3 in Par1 and $G\alpha_{q/11}$-dependent manner and down-regulation of PLCβ3 negates thrombin-induced LMCD1 and CDC6 expression and DNA synthesis suggest that PLCβ3 acts downstream to Par1 and $G\alpha_{q/11}$ in the mediation of LMCD1-dependent CDC6 expression in enhancing HASMC replication by thrombin. Interestingly thrombin-induced MASMC or RASMC growth does not require LMCD1. Because down-regulation of LMCD1 blocks both PDGF-BB and thrombin-induced DNA synthesis only in HASMC but not MASMC or RASMC, it is likely that the role of LMCD1 in CDC6 expression and DNA synthesis is selective for humans. The lack of the effect of mouse

common carotid artery ligation or rat carotid artery BI on LMCD1 induction while increasing the levels of E2F1 and CDC6 further supports a disconnect between LMCD1 and E2F1 in the induction of CDC6 expression in the modulation of rodent VSMC growth *in vivo* as well. It should be pointed out that E2F1 mediates CDC6 expression in the induction of DNA synthesis in rat embryonic fibroblasts (17). However, it was also reported that the selectivity of various E2Fs on CDC6 expression in inducing DNA synthesis in mammalian cells depends on their interaction with factors such as YY1 (35). Based on these observations, it may be suggested that various E2Fs via interacting with distinct other factors such as LMCD1 or YY1 attain selectivity in mediating CDC6 expression in the induction of DNA synthesis in response to a specific agonist in a particular cell type. The link between LMCD1 and E2F1 in CDC6 expression in the modulation of VSMC replication in human atherosclerotic lesions is consistent with its role in the regulation HASMC multiplication *in vitro*. Based on these observations and the fact that VSMC growth is an important contributing factor in restenosis, one can postulate that LMCD1 via enhancing VSMC proliferation influences the development of neointima in humans but not rodents. Because VSMC multiplication is a common factor in restenosis and during the early development of atherosclerosis (24, 36), the above observations further infer that LMCD1 via enhancing VSMC replication can promote the pathogenesis of atherosclerosis as well. In addition, on the basis of the present observations, it may be suggested that although thrombin modulates the growth of both rodent and human VSMCs (7, 8, 30), it might be mediating these effects by engaging distinct signaling events in different species. Therefore, the observations made by studies involving animals may require caution to extrapolate them to humans and thus warrant species-specific studies to understand the human disease process and to develop the targeted therapeutic molecules.

As summarized in Fig. 8, the present findings demonstrate that LMCD1 acts as a co-activator for E2F1 in the regulation of CDC6 expression mediating human but not mouse or rat aortic smooth muscle cell replication in response to a GPCR agonist, thrombin, involving Par1, $G\alpha_{q/11}$, and PLCβ3. On the basis of these observations, it is likely that LMCD1 plays a role in restenosis in humans. In addition, the present observations suggest that LMCD1 via enhancing SMC replication may promote SMC-derived foam cell formation and hence influence atherogenesis in humans.

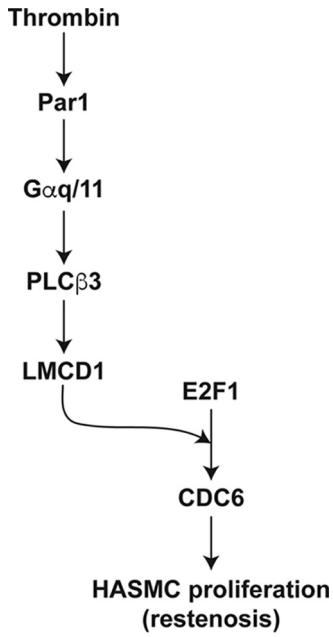

Figure 8. Schematic diagram depicting the potential signaling of LMCD1-mediated CDC6 expression in the induction of human aortic smooth muscle cell replication by thrombin.

Materials and methods

Reagents

Anti-CDC6 (SC-9964), anti-CDK4 (SC-260), anti-DDK tag (SC-166384), anti-E2F1 (SC-251), anti-Gαq (SC-393), anti-Gα11 (SC-390382), anti-Gα12 (SC-409), anti-Gα13 (SC-410), anti-HA-tag (SC-53516, SC-57592), anti-MCM2 (SC-9839), anti-MCM3 (SC-9850), anti-MCM4 (SC-28317), anti-MCM5 (SC-136366), anti-MCM6 (SC-9843), anti-MCM7 (SC-9966), anti-Myc tag (SC-789; SC-40), anti-Par1 (SC-13503), anti-PLCβ1 (SC-205), anti-PLCβ2 (SC-9018), anti-PLCβ3 (SC-403), anti-PLCβ4 (SC-404), and anti-β-Tubulin (SC-9104) antibodies and Duolink *in situ* PLA reagents were obtained from Santa Cruz Biotechnology (Santa Cruz, CA). Anti-LMCD1 antibodies (ab179454) and TUNEL Assay Kit (ab66110) were bought from Abcam (Cambridge, MA). Duolink *in situ* PLA reagents were procured from Sigma–Aldrich. SCH79797 was obtained from TOCRIS Biosciences (Bristol, UK). pGL3 basic vector and Luciferase assay system (E4530) were purchased from Promega (Madison, WI). Biotin 3′-end DNA labeling kit (89818) and light-shift chemiluminescent EMSA kit (20148) were procured from Pierce Biotechnology. Human $G\alpha_q$ siRNA (ON-TARGETplus SMARTpool J-008562), human $G\alpha_{11}$ siRNA (ON-TARGETplus SMARTpool J-010860), and control nontargeting siRNA (D-001810-10) were purchased from Dharmacon RNAi Technologies (Chicago, IL). Goat anti-rabbit HRP (31460) and goat anti-mouse HRP (31437) antibodies, Lipofectamine 3000 transfection reagent (L3000–015), Hoechst 33342 (H3570), Prolong gold antifade mounting medium (P36930), medium 231 (M231-500), smooth muscle growth supplements (S-007-25), and gentamicin/amphotericin solution (R-015-10) were obtained from Thermo Scientific (Waltham, MA). Protein A-Sepharose CL-4B (170780-01), protein G-Sepharose Fast flow (17061801), and ECL Western blotting detection reagents (RPN2106) were purchased from GE Healthcare.

Primers

All the primers for RT-PCR, cloning, EMSA, and ChIP were synthesized by IDT (Coralville, IA) and listed in Table 1.

Cell culture

HASMCs were obtained from Invitrogen and subcultured in medium 231 containing smooth muscle cell growth supplements and gentamicin/amphotericin at 37 °C in humidified 95% air-5% CO_2 atmosphere. The cells with passage numbers between 4 and 10 were growth-arrested in medium 231 without

Table 1
List of primers used in the study

	Forward primer (5′ → 3′)	Reverse primer (5′ → 3′)
Primers used for mRNA amplification by RT-PCR		
ANXA10	GCCTGAGTCTGAGGTGAACA	TGTCACAGTCAAATCCTTGGAG
BMP2	AGAATAACTTGCGCACCCCA	GAGACCGCAGTCCGTCTAAG
DIRAS3	GAGAAAGGGGTCTCCTGCT	GTGCAGCAGCGTACTTTTCC
DUSP1	CACTCTACGATCAGGGTGGC	GGAGCTGATGTCTGCCTTGT
GABBR2	GAACTGGCCATCGAGCAGA	GCAGCAAAAGAAAGCTGCAC
HAS2	ACCAAGAGCTGAACAAGATGC	CGGTGCTCCAAAAAGGCAAA
LMCD1	ACAGAGGGTGCCTTTTACCG	GCTCGCAGACGTATTCCACT
PAR2	AGTGGCACCATCCAAGGAAC	GCAAACCCACCACAAACACA
RGS4	TCATGAATGTGAACCTGGATTCTTG	TGGCATTTCATCCCTCTGCC
SERPINB2	TGGCCAAGGTGCTTCAGTTTA	GCAGACTTCTCACCAAACAGC
SERPINE1	GACCTCAGGAAGCCCCTAGA	ACTGTTCCTGTGGGGTTGTG
SOCS2	GACTTCAAGGAAGGACGCGA	CCCCAGTACCATCCTGTCTG
STC1	AACTCAGCTGAAGTGGTTCGT	GAAAGTGGAGCACCTCCGAA
TIMP3	CAGTACCTGCTGACAGGTCG	AGGCGTAGTGTTTGGACTGG
TMEM158	GGGCCCTTTCCCCTCTATTG	AAATCCTTCCCATGCCCTCC
TNFRSF12A	GAGAAGTTCACCACCCCCAT	ACCTTGGAAGGTTCCCCTGA
XYLT1	TGCTTCCTGCTGAGTCCTTC	TCCTGATTCACCACGGCTTC
CDC6	AGAAGGGCCCCATGATTGTG	TGCAGCATTGTCCAGAACCT
Primers used for human CDC6 promoter cloning into pGL3 basic vector		
CDC6p (1.2 kb)	ATAAGAGCTCCTGGCATACACTTAAGCACTCAATA	CGTTAAGCTTCTTCTCACGTCTCTCACAC
CDC6p (0.6 kb)	ATAAGAGCTCATCACTAGTTCAGCCATCAGGAGATC	
CDC6p (0.4 kb)	ATAAGAGCTCGAACCACATCTTGACACTTCCAG	
CDC6p (0.2 kb)	ATAAGAGCTCCGTTCAGTGGTCGTGGCCTCA	
CDC6p (0.1 kb)	ATAAGAGCTCTGGGAACGCTGTGGCCATT	
CDC6p-E2F (Mut)	GAGGCCGGGCTTTGAAGGGAGGTGGGAACG	CGTTCCCACCTCCCTTCAAAGCCCGGCCTC
Primers used for EMSA		
CDC6-E2F-(WT)	AATCGAGGCCGGGCT[b]TTGGCGGGAGGTGGGAA	TTCCCACCTC[b]CCGCCAAAGCCCGGCCTCGATT
CDC6-E2F-(Mut)	AATCGAGGCCGGGCAATT[bi]CCGGGAGGTGGGAA	TTCCCACCTC[bi]CCGGAATTGCCCGGCCTCGATT
Primer used for ChIP assay		
CDC6-E2F	AAAAGAGGCGGTGCCCAAGG	CACCACCACAAGCCCCTGAAC
Primers used for gene cloning		
Cys-PET-LIM1	AGTCTGCGGCCCACGCGTACGCGG	CCGCGTACGCGTGGGCCGCAGACT
PET-LIM1-LIM2	CAGCAAGAGGTGTGGCACTAACATCTGACCTAGA	TCTAGGTCAGATGTTAGTGCCACACCTCTTGCTG
Cys-PET	CGCGTACGCGTTTCCACTTCTTTGGACGGGTC	GACCCGTCCAAAGAAGTGGAAACGCGTACGCG
PET	TCTAGGTCAGATGTTAGTGCCACACCTCTTGCTG	GCAAGAGGTGTGGCATTGCCCAAGGAGGAG
LIM1-LIM2	GCAAGAGGTGTGGCATTGCCCAAGGAGGAG	CTCCTCCTTGGGCAATGCCACACCTCTTGC
LIM1	AGTCTGCGGCCCACGCGTACGCGG	CCGCGTACGCGTGGGCCGCAGACT
LIM2	CCCGTCCAAAGAAGTGGAACGGTGCTCCG	CGGAGCACCGTTCCACTTCTTTGGACGGG
PET-LIM1	AGTCTGCGGCCCACGCGTACGCGG	CCGCGTACGCGTGGGCCGCAGACT
PET-LIM2	CCCGTCCAAAGAAGTGGAACGGTGCTCCG	CGGAGCACCGTTCCACTTCTTTGGACGGG
E2F1 (1–317 AA)[a]	CCCATCCCAGGAGGTCACTTGATCTGAGGAGG	CCTCCTCAGATCAAGTGACCTCCTGGGATGGG
E2F1 (1–243 AA)	CACTGACAGCCAGTGACGCCTGGCCTACG	CGTAGGCCAGGCGTCACTGGCTGTCAGTG
E2F1 (1–191 AA)	TCATGCATCCTGTCAGCTGCCCAGCCACTG	CAGTGGCTGGGCAGCTGACAGGATGCATGA
E2F1 (318–437 AA)	TGTTCTCCTCCTCAGACATATGGGATCCGAGG	CCTCGGATCCCATATGTCTGAGGAGGAGAACA

[a] AA, amino acids.

any growth supplements overnight and used for the experiments unless otherwise indicated.

Microarray analysis

Quiescent HASMCs were treated with and without thrombin (0.5 unit/ml) for the indicated time periods, and total cellular RNA was extracted by TRIzol reagent, purified using Qiagen RNeasy mini kit, and sent for microarray analysis to SABiosciences (human HT-12v4 expression bead chip assay). The heat map was generated by using R statistical programming software. The gene ontology analysis was performed in the Panther classification system (www.pantherdb.org).[3] The microarray data has been submitted to the Gene Expression Omnibus (code GSE104498).

Animals

Sprague-Dawley rats and C57BL/6 mice were obtained from Charles River Laboratories (Wilmington, MA) and maintained at the University of Tennessee Health Science Center's animal facilities. All the experiments involving animals were performed according to protocols approved by the Institutional Animal Care and Use Committee of the University of Tennessee Health Science Center (Memphis, TN).

Human normal and atherosclerotic artery specimen

All human normal and atherosclerotic artery samples were collected as described previously following the protocols approved by the institutional review boards (37). These samples were considered to be deemed nonhuman subjects, because they were postmortem samples. Both genders were used with age groups ranging from 21 to 71 years.

Co-immunoprecipitation

After rinsing with cold PBS, the cells were lysed in 400 μl of lysis buffer (PBS, 1% Nonidet P-40, 0.5% sodium deoxycholate, 0.1% SDS, 100 μg/ml PMSF, 100 μg/ml aprotinin, 1 μg/ml leupeptin, and 1 mM sodium orthovanadate) for 20 min on ice. The cell extracts were cleared by centrifugation at 14,000 rpm for 20 min at 4 °C. The cleared cell extracts containing an equal

[3] Please note that the JBC is not responsible for the long-term archiving and maintenance of this site or any other third party hosted site.

amount of protein from control, and the indicated treatments were incubated with the indicated antibodies overnight at 4 °C, followed by incubation with protein A/G-Sepharose CL4B beads for 3 h with gentle rocking. The beads were collected by centrifugation at 1000 rpm for 2 min at 4 °C and washed four times with lysis buffer and once with PBS. The immunocomplexes were released by heating the beads in 40 μl of Laemmli sample buffer and analyzed by Western blotting for the indicated molecules using their specific antibodies.

Apoptosis

Apoptosis was measured using TUNEL assay kit following the manufacturer's instructions.

DNA synthesis

DNA synthesis was measured by [^{3}H]thymidine incorporation as described previously (38) and expressed as counts/min/dish.

Western blotting

Equal amounts of protein from control and treatment samples were separated by SDS-PAGE and analyzed by Western blotting for the indicated molecules using their specific antibodies as described previously with minor modifications (23). Briefly, all the primary antibodies were used at 1:500 to 1:1000 dilutions and incubated overnight at 4 °C. Goat anti-rabbit or goat anti-mouse antibodies conjugated with HRP were used at 1:4000 to 1:5000 dilutions and incubated for 2 h at room temperature. The blots were developed using ECL detection reagents and quantified by densitometry using ImageJ software (National Institutes of Health).

Cloning and site-directed mutagenesis

Human LMCD1 overexpression plasmid (Myc-DDK-tagged pCMV6-LMCD1) was obtained from Origene (catalog no. RC200062). Human E2F1 overexpression plasmid (HA-tagged pRcCMV-E2F1) was a gift from Dr. William Kaelin (Addgene plasmid catalog no. 21667) (39). LMCD1 and E2F1 truncates were made from pCMV6-LMCD1 and pRcCMV-E2F1 plasmids, respectively, using the QuikChange Lightning Site-directed mutagenesis kit (Agilent Technologies; catalog no. 210518) and the primers listed in Table 1. Human CDC6 promoter with various truncations were cloned into pGL3 basic vector using the primers listed in Table 1. Mutation in the E2F at −43 nt was introduced by the QuikChange Lightning site-directed mutagenesis kit. Plasmid DNAs were purified using the EndoFree plasmid maxi kit (catalog no. 12362; Qiagen) and used in the transfection experiments.

Transfections

HASMCs were transfected with nontargeted control or on-target siRNA at a final concentration of 100 nM using Lipofectamine 3000 transfection reagent according to the manufacturer's instructions. The cells were transfected with plasmid DNAs at a final concentration of 2.5 μg/60-mm dish or 5 μg/100-mm dish using Lipofectamine 3000 transfection reagent according to the manufacturer's instructions. After transfections, the cells were growth-arrested for 36 h and used as required.

EMSA

Nuclear extracts of HASMCs with and without appropriate treatments were prepared using NE-PER nuclear and cytoplasmic extraction reagents according to the manufacturer's (catalog no. 78833, Thermo Scientific) instructions. The protein content of the nuclear extracts was determined using a micro-BCA method (Pierce Biotechnology). Biotin-labeled double-stranded oligonucleotides encompassing E2F-binding element at −43 nt with forward (CDC6-E2F-WT_F) and reverse (CDC6-E2F-WT_R) as WT probe and forward (CDC6-E2F-Mu_F) and reverse (CDC6-E2F-Mu_R) as mutant probe were used. Briefly, 5 μg of nuclear extract was incubated in a binding buffer (10 mM Tris-HCl, pH 7.5, 50 mM KCl, 1 mM DTT, 2.5% glycerol) with 2.5 nM of biotin-labeled probe and 2 μg of poly(dI·dC) for 30 min at room temperature in a total volume of 20 μl on ice, and the DNA–protein complexes were resolved by electrophoresis on a 6% polyacrylamide gel using Tris borate–EDTA buffer (44.5 mM Tris-HCl, 44.5 mM borate, and 20 mM EDTA, pH 8.0). After separation the protein–DNA complexes were transferred to nylon membrane using Tris borate–EDTA buffer, UV cross-linked, and visualized by chemiluminescence. To perform a supershift EMSA, the complete reaction mix was incubated with 2 μg of the indicated antibody for 1 h on ice before separating it by electrophoresis. Normal serum was used as a negative control.

Luciferase assay

HASMCs were co-transfected with pGL3 empty vector, pGL3-hCDC6, or pGL3-hCDC6m promoter along with the indicated plasmids using Lipofectamine 3000 transfection reagent. After growth arresting in serum-free medium for 36 h, the cells were treated with and without 0.5 unit of thrombin or 6 h, washed with cold PBS, and lysed in 200 μl of lysis buffer. The cell extracts were cleared by centrifugation at 12,000 rpm for 2 min at 4 °C. The supernatants were assayed for luciferase activity using luciferase assay system (Promega) and a single tube luminometer (TD20/20; Turner Designs, Sunnyvale, CA) and expressed as relative luciferase units.

ChIP

HASMCs with and without the indicated treatments were fixed with 1% formaldehyde for 10 min at 37 °C, washed, and scraped in PBS and centrifuged at 2000 rpm for 4 min at 4 °C to pellet the cells. The cell pellet was resuspended in SDS lysis buffer (1% SDS, 10 mM EDTA, 50 mM Tris-HCl, pH 8.1) containing protease inhibitors (1 μg/ml aprotinin, 1 μg/ml pepstatin, and 1 mM PMSF), sonicated, centrifuged at 13,000 rpm for 10 min at 4 °C, and collected the supernatant. The supernatant was diluted with ChIP dilution buffer (16.7 mM Tris-HCl, pH 8.1, 167 mM NaCl, 1.2 mM EDTA, 0.01% SDS, and 1.1% Triton X-100) and immunoprecipitated with anti-LMCD1 or anti-E2F1 antibodies. Mouse or rabbit preimmune serum was used as a negative control. For re-ChIP assay, the chromatin complexes were eluted from the first ChIP with 10 mM DTT at 37 °C for 30 min, diluted 20 times with ChIP dilution buffer,

and immunoprecipitated with the indicated antibodies. The immunoprecipitated DNA was un-cross-linked, subjected to proteinase K digestion, and purified using QIAquick columns (catalog no. 28104, Qiagen). The ChIP and re-ChIP samples were analyzed by PCR using the ChIP-E2F_F and ChIP-E2F_R primers that would amplify a 165-bp fragment encompassing the E2F-binding site at −43 nt.

In situ PLA

The interaction between endogenous LMCD1 and E2F1 was analyzed by using *in situ* proximity ligation assay kit (Duolink PLA kit; Sigma) following the manufacturer's instructions. Briefly, after appropriate treatments, HASMCs were fixed with 3.7% paraformaldehyde for 15 min, permeabilized in 0.3% Triton X-100 for 15 min, and blocked with 3% BSA for 1 h. The cells were then incubated with mouse anti-E2F1 (1:100) and rabbit anti-LMCD1 (1:200) antibodies overnight at 4 °C followed by incubation with goat anti-mouse secondary antibody conjugated with oligonucleotide PLA probe Plus and goat anti-rabbit secondary antibody conjugated with oligonucleotide PLA probe Minus, respectively. The cells were then incubated with a ligation solution for 30 min at 37 °C followed by a rolling-circle amplification of ligated oligonucleotide probes. A fluorescently labeled complementary oligonucleotide detection probe was used to amplify the oligonucleotides conjugated to the secondary antibodies. After washing with wash buffer, the slides were mounted with a mounting medium containing 4′,6′-diamino-2-phenylindole. PLA signals were examined using a Zeiss 710 NLO multi-photon microscope (magnification at 20×/1.0 NA), and the fluorescence intensities were captured with ZEN operating software (Lasers 405 and 543).

Immunofluorescence

The human normal and atherosclerotic artery sections were deparaffinized with xylene and then treated with antigen-unmasking solution for 15 min at 99 °C. The sections were permeabilized with 0.5% Triton X-100 for 15 min, and after blocking in normal goat serum, the sections were probed with mouse anti-mouse SMCα-actin and rabbit anti-human LMCD1 (Alexa Fluor 568-conjugated antibody) in combination with rabbit anti-human Ki67 or rabbit anti-human CDC6 (all at 1:100 dilution) or filipin, followed by incubation with Alexa Fluor 488-conjugated goat anti-mouse or Alexa Fluor 350-conjugated goat anti-mouse and Alexa Fluor 488-conjugated goat anti-rabbit secondary antibodies (all at 1:500 dilution). The sections were observed under a Zeiss Inverted Microscope (Zeiss AxioObserver Z1; magnification at 40×/NA 0.6), and the fluorescence images were captured with a Zeiss AxioCam MRm camera using the microscope operating software and Image Analysis Software AxioVision 4.7.2 (Carl Zeiss Imaging Solutions).

Balloon injury (BI) and carotid artery ligation (CAL)

BI was performed essentially as described previously (30). At 5 days post-BI, the animals were sacrificed with an overdose of ketamine/xylazine (200 mg/kg), and the carotid arteries were isolated. The arteries were cleaned, and tissue extracts were prepared for further analysis. To perform CAL, the mice were anesthetized with ketamine/xylazinem, and the right common carotid artery was exposed and ligated with a 6-0 Ethicon suture just proximal to the carotid artery bifurcation (40). The surgical incision was closed, and the mice were maintained in the animal facilities. At 1 week post-CAL, the mice were euthanized with an overdose of ketamine/xylazine (200 mg/kg), the ligated arteries were isolated, and tissue extracts were prepared for further analysis.

Statistics

All the experiments were repeated three times, and the data are presented as means ± S.D. Two-way analysis of variance was used to perform statistical analysis, and p values < 0.05 were considered statistically significant. In the case of EMSA, supershift EMSA, *in situ* PLA, and Western blotting, one representative set of data is shown.

Author contributions—J. J., B. Z., A. M. M., and N. K. S. data curation; J. J., B. Z., A. M. M., and G. N. R. formal analysis; J. J., B. Z., A. M. M., and G. N. R. validation; J. J., B. Z., and A. M. M. methodology; J. G. T., A. W. O., and G. N. R. resources; G. N. R. conceptualization; G. N. R. supervision; G. N. R. funding acquisition; G. N. R. project administration; G. N. R. writing-review and editing.

References

1. Liu, M. W., Roubin, G. S., and King, S. B., 3rd (1989) Restenosis after coronary angioplasty: potential biologic determinants and role of intimal hyperplasia. *Circulation* **79,** 1374–1387 CrossRef Medline
2. Bauters, C., and Isner, J. M. (1997) The biology of restenosis. *Prog. Cardiovasc. Dis.* **40,** 107–116 CrossRef Medline
3. Berk, B. C. (2001) Vascular smooth muscle growth: autocrine growth mechanisms. *Physiol. Rev.* **81,** 999–1030 CrossRef Medline
4. Walz, D. A., Anderson, G. F., Ciaglowski, R. E., Aiken, M., and Fenton, J. W., 2nd (1985) Thrombin-elicited contractile responses of aortic smooth muscle. *Proc. Soc. Exp. Biol. Med.* **180,** 518–526 CrossRef Medline
5. Wilner, G. D., Danitz, M. P., Mudd, M. S., Hsieh, K. H., and Fenton, J. W., 2nd (1981) Selective immobilization of alpha-thrombin by surface-bound fibrin. *J. Lab. Clin. Med.* **97,** 403–411 Medline
6. Bar-Shavit, R., Kahn, A., Fenton, J. W., 2nd, and Wilner, G. D. (1983) Chemotactic response of monocytes to thrombin. *J. Cell Biol.* **96,** 282–285 CrossRef Medline
7. McNamara, C. A., Sarembock, I. J., Gimple, L. W., Fenton, J. W., 2nd, Coughlin, S. R., and Owens, G. K. (1993) Thrombin stimulates proliferation of cultured rat aortic smooth muscle cells by a proteolytically activated receptor. *J. Clin. Invest.* **91,** 94–98 CrossRef Medline
8. Rauch, B. H., Millette, E., Kenagy, R. D., Daum, G., Fischer, J. W., and Clowes, A. W. (2005) Syndecan-4 is required for thrombin-induced migration and proliferation in human vascular smooth muscle cells. *J. Biol. Chem.* **280,** 17507–17511 CrossRef Medline
9. Bespalova, I. N., and Burmeister, M. (2000) Identification of a novel LIM domain gene, *LMCD1*, and chromosomal localization in human and mouse. *Genomics* **63,** 69–74 CrossRef Medline
10. Kadrmas, J. L., and Beckerle, M. C. (2004) The LIM domain: from the cytoskeleton to the nucleus. *Nat. Rev. Mol. Cell Biol.* **5,** 920–931 CrossRef Medline
11. Bian, Z. Y., Huang, H., Jiang, H., Shen, D. F., Yan, L., Zhu, L. H., Wang, L., Cao, F., Liu, C., Tang, Q. Z., and Li, H. (2010) LIM and cysteine-rich domains 1 regulates cardiac hypertrophy by targeting calcineurin/nuclear factor of activated T cells signaling. *Hypertension* **55,** 257–263 CrossRef Medline
12. Rath, N., Wang, Z., Lu, M. M., and Morrisey, E. E. (2005) LMCD1/Dyxin is a novel transcriptional cofactor that restricts GATA6 function by inhibiting DNA binding. *Mol. Cell. Biol.* **25,** 8864–8873 CrossRef Medline

13. Lepore, J. J., Cappola, T. P., Mericko, P. A., Morrisey, E. E., and Parmacek, M. S. (2005) GATA-6 regulates genes promoting synthetic functions in vascular smooth muscle cells. *Arterioscler. Thromb. Vasc. Biol.* **25,** 309–314 Medline
14. Perlman, H., Suzuki, E., Simonson, M., Smith, R. C., and Walsh, K. (1998) GATA-6 induces p21(Cip1) expression and G_1 cell cycle arrest. *J. Biol. Chem.* **273,** 13713–13718 CrossRef Medline
15. Cocker, J. H., Piatti, S., Santocanale, C., Nasmyth, K., and Diffley, J. F. (1996) An essential role for the Cdc6 protein in forming the pre-replicative complexes of budding yeast. *Nature* **379,** 180–182 CrossRef Medline
16. Speck, C., and Stillman, B. (2007) Cdc6 ATPase activity regulates ORC x Cdc6 stability and the selection of specific DNA sequences as origins of DNA replication. *J. Biol. Chem.* **282,** 11705–11714 CrossRef Medline
17. Ohtani, K., Tsujimoto, A., Ikeda, M., and Nakamura, M. (1998) Regulation of cell growth-dependent expression of mammalian CDC6 gene by the cell cycle transcription factor E2F. *Oncogene* **17,** 1777–1785 CrossRef Medline
18. Chen, T. C., Lin, K. T., Chen, C. H., Lee, S. A., Lee, P. Y., Liu, Y. W., Kuo, Y. L., Wang, F. S., Lai, J. M., and Huang, C. Y. (2014) Using an *in situ* proximity ligation assay to systematically profile endogenous protein–protein interactions in a pathway network. *J. Proteome Res.* **13,** 5339–5346 CrossRef Medline
19. Ma, L., Perini, R., McKnight, W., Dicay, M., Klein, A., Hollenberg, M. D., and Wallace, J. L. (2005) Proteinase-activated receptors 1 and 4 counter-regulate endostatin and VEGF release from human platelets. *Proc. Natl. Acad. Sci. U.S.A.* **102,** 216–220 CrossRef Medline
20. Kelley, G. G., Kaproth-Joslin, K. A., Reks, S. E., Smrcka, A. V., and Wojcikiewicz, R. J. (2006) G-protein-coupled receptor agonists activate endogenous phospholipase Cϵ and phospholipase Cβ3 in a temporally distinct manner. *J. Biol. Chem.* **281,** 2639–2648 CrossRef Medline
21. Lyon, A. M., Begley, J. A., Manett, T. D., and Tesmer, J. J. (2014) Molecular mechanisms of phospholipase C β3 autoinhibition. *Structure* **22,** 1844–1854 CrossRef Medline
22. Huang, W., Hicks, S. N., Sondek, J., and Zhang, Q. (2011) A fluorogenic, small molecule reporter for mammalian phospholipase C isozymes. *ACS Chem. Biol.* **6,** 223–228 CrossRef Medline
23. Janjanam, J., Chandaka, G. K., Kotla, S., and Rao, G. N. (2015) PLCβ3 mediates cortactin interaction with WAVE2 in MCP1-induced actin polymerization and cell migration. *Mol. Biol. Cell* **26,** 4589–4606 CrossRef Medline
24. Ip, J. H., Fuster, V., Badimon, L., Badimon, J., Taubman, M. B., and Chesebro, J. H. (1990) Syndromes of accelerated atherosclerosis: role of vascular injury and smooth muscle cell proliferation. *J. Am. Coll. Cardiol.* **15,** 1667–1687 CrossRef Medline
25. Allahverdian, S., Chehroudi, A. C., McManus, B. M., Abraham, T., and Francis, G. A. (2014) Contribution of intimal sooth muscle cells to cholesterol accumulation and macrophage-like cells in human atherosclerosis. *Circulation* **129,** 1551–1559 CrossRef Medline
26. Johnson, J. L. (2014) Emerging regulators of vascular smooth muscle cell function in the development and progression of atherosclerosis. *Cardiovasc. Res.* **103,** 452–460 CrossRef Medline
27. Chellan, B., Reardon, C. A., Getz, G. S., and Hofmann Bowman, M. A. (2016) Enzymatically modified low-density lipoprotein promotes foam cell formation in smooth muscle cells via macropinocytosis and enhances receptor-mediated uptake of oxidized low-density lipoprotein. *Arterioscler. Thromb. Vasc. Biol.* **36,** 1101–1113 CrossRef Medline
28. Ballantyne, M. D., Pinel, K., Dakin, R., Vesey, A. T., Diver, L., Mackenzie, R., Garcia, R., Welsh, P., Sattar, N., Hamilton, G., Joshi, N., Dweck, M. R., Miano, J. M., McBride, M. W., Newby, D. E., *et al.* (2016) Smooth muscle enriched long noncoding RNA (SMILR) regulates cell proliferation. *Circulation* **133,** 2050–2065 CrossRef Medline
29. Karpurapu, M., Wang, D., Singh, N. K., Li, Q., and Rao, G. N. (2008) NFATc1 targets cyclin A in the regulation of vascular smooth muscle cell multiplication during restenosis. *J. Biol. Chem.* **283,** 26577–26590 CrossRef Medline
30. Wang, D., Paria, B. C., Zhang, Q., Karpurapu, M., Li, Q., Gerthoffer, W. T., Nakaoka, Y., and Rao, G. N. (2009) A role for Gab1/SHP2 in thrombin activation of PAK1: gene transfer of kinase-dead PAK1 inhibits injury-induced restenosis. *Circ. Res.* **104,** 1066–1075 CrossRef Medline
31. Kundumani-Sridharan, V., Singh, N. K., Kumar, S., Gadepalli, R., and Rao, G. N. (2013) Nuclear factor of activated T cells c1 mediates p21-activated kinase 1 activation in the modulation of chemokine-induced human aortic smooth muscle cell F-actin stress fiber formation, migration, and proliferation and injury-induced vascular wall remodeling. *J. Biol. Chem.* **288,** 22150–22162 CrossRef Medline
32. Louie, M. C., Zou, J. X., Rabinovich, A., and Chen, H. W. (2004) ACTR/AIB1 functions as an E2F1 coactivator to promote breast cancer cell proliferation and antiestrogen resistance. *Mol. Cell. Biol.* **24,** 5157–5171 CrossRef Medline
33. Tanski, W. J., Roztocil, E., Hemady, E. A., Williams, J. A., and Davies, M. G. (2004) Role of $G\alpha_q$ in smooth muscle cell proliferation. *J. Vasc. Surg.* **39,** 639–644 CrossRef Medline
34. Austin, K. M., Nguyen, N., Javid, G., Covic, L., and Kuliopulos, A. (2013) Noncanonical matrix metalloprotease-1-protease-activated receptor-1 signaling triggers vascular smooth muscle cell dedifferentiation and arterial stenosis. *J. Biol. Chem.* **288,** 23105–23115 CrossRef Medline
35. Schlisio, S., Halperin, T., Vidal, M., and Nevins, J. R. (2002) Interaction of YY1 with E2Fs, mediated by RYBP, provides a mechanism for specificity of E2F function. *EMBO J.* **21,** 5775–5786 CrossRef Medline
36. Chen, K. H., Guo, X., Ma, D., Guo, Y., Li, Q., Yang, D., Li, P., Qiu, X., Wen, S., Xiao, R. P., and Tang, J. (2004) Dysregulation of HSG triggers vascular proliferative disorders. *Nat Cell Biol.* **6,** 872–883 CrossRef Medline
37. Funk, S. D., Yurdagul, A., Jr., Albert, P., Traylor, J. G., Jr., Jin, L., Chen, J., and Orr, A. W. (2012) EphA2 activation promotes the endothelial cell inflammatory response: a potential role in atherosclerosis. *Arterioscler. Thromb. Vasc. Biol.* **32,** 686–695 CrossRef Medline
38. Rao, G. N., Katki, K. A., Madamanchi, N. R., Wu, Y., and Birrer, M. J. (1999) JunB forms the majority of the AP-1 complex and is a target for redox regulation by receptor tyrosine kinase and G protein-coupled receptor agonists in smooth muscle cells. *J. Biol. Chem.* **274,** 6003–6010 CrossRef Medline
39. Krek, W., Ewen, M. E., Shirodkar, S., Arany, Z., Kaelin, W. G., Jr., and Livingston, D. M. (1994) Negative regulation of the growth-promoting transcription factor E2F-1 by a stably bound cyclin A-dependent protein kinase. *Cell* **78,** 161–172 CrossRef Medline
40. Wang, D., Oparil, S., Chen, Y. F., McCrory, M. A., Skibinski, G. A., Feng, W., and Szalai, A. J. (2005) Estrogen treatment abrogates neointima formation in human C-reactive protein transgenic mice. *Arterioscler. Thromb. Vasc. Biol.* **25,** 2094–2099 CrossRef Medline